Fluid transport equation in porous media (Fluid compressibility)

Conservation law of mass:

$$\frac{\partial \rho_\phi}{\partial t} + \nabla \cdot (\rho \vec{v}) = 0$$

$$\phi - Poracity(constant, 0 < \phi < 1)$$

Darcy's law:

$$\vec{v} = -\frac{k}{\mu}\nabla p \quad \text{(2-D flow)}$$

$$\Rightarrow \phi \frac{\partial p}{\partial t} + \nabla(-\frac{k}{\mu}\rho \nabla p) = 0$$

State equation(fluid):

$$c \cdot dp = \frac{d\rho}{\rho} \quad \text{(c-modulus of elasticity)}$$

$$\Rightarrow c\phi \frac{\partial p}{\partial t} - \nabla(\frac{k}{\mu}\nabla p) - c\frac{k}{\mu}|\nabla p|^2 = 0 \quad (c \ll 1)$$

$$\Rightarrow c\phi \frac{\partial p}{\partial t} - \nabla(\frac{k}{\mu}\nabla p) = 0$$

Initial condition:

$$p|_{t=0} = p_0 \quad (p_0 \text{ is constant})$$

Boundary condition :on Γ_w(well)

$$p|_{\Gamma_w} = p_w \quad (p_w \text{ is constant unknown})$$

$$\int_{\Gamma_w} \vec{v} \cdot \vec{n}\, ds = L \quad (\vec{n}\ is\ outer\ normal \quad L\ is\ volume\ of\ product)$$

$$h\int_0^{2\pi} -\frac{k}{\mu}(-\frac{\partial p}{\partial r})r\ ds) = Q \quad (h\ is\ thickness)$$

$$(r\frac{\partial p}{\partial r})|_{\Gamma_w} = \frac{Q\mu}{2\pi k h}$$

radius $r_w \ll 1$

$$\lim_{r_w \to 0} (r\frac{\partial p}{\partial r})|_{\Gamma_w} = \frac{Q\mu}{2\pi k h}$$

Problem

Find $p(r,t)$ s.t.

$$\begin{cases} \phi c \frac{\partial p}{\partial t} = \frac{1}{r}\frac{\partial}{\partial r}(\frac{k}{\mu} r(\frac{\partial p}{\partial r})) & (r > 0) \\ \lim_{r \to 0}(r\frac{\partial p}{\partial r})) = \frac{Q\mu}{2\pi k h} \\ p|_{t=0} = p_0 \end{cases}$$

rescale

$$\begin{cases} \frac{\partial p}{\partial t} = \frac{1}{r}\frac{\partial}{\partial r}(kr(\frac{\partial p}{\partial r})) & (r > 0) \\ \lim_{r \to 0}(r\frac{\partial p}{\partial r}) = Q \\ p|_{t=0} = p_0 \end{cases}$$

Solution

$$P(r,t) = p_0 - \frac{Q}{2}\int_{\frac{r^2}{4kt}}^{\infty} \frac{e^{-\lambda}}{\lambda}\, d\lambda$$

Permeability k:

$k = 1 \qquad \frac{\partial p}{\partial r} = |\nabla p| > \mu$

$k = 0 \qquad \frac{\partial p}{\partial r} = |\nabla p| < \mu$

$(\mu > 0)$

$k = H(\frac{\partial p}{\partial r} - \mu)$

$$\begin{cases} \frac{\partial p}{\partial t} = \frac{1}{r}\frac{\partial}{\partial r}(rH(\frac{\partial p}{\partial r} - \mu)\frac{\partial p}{\partial r}) \\ \lim_{r \to 0}(r\frac{\partial p}{\partial r}) = Q \\ p|_{t=0} = p_0 \end{cases} \qquad (*)$$

In Song Fuquan's paper

permeability

$$k = (1 - \frac{\mu}{|\nabla p|})^+ = (1 - \frac{\mu}{\frac{\partial p}{\partial r}})^+$$

Now we consider another appoximation for equation (*)

There is a boundary layer near $\Gamma : \{\frac{\partial p}{\partial r} = \mu\}$

$\frac{\partial p}{\partial r}: \quad \mu + \delta \searrow \mu$

$k: \quad 1 \quad \searrow 0$

$k = k_\delta(\frac{\partial p}{\partial r}) =$

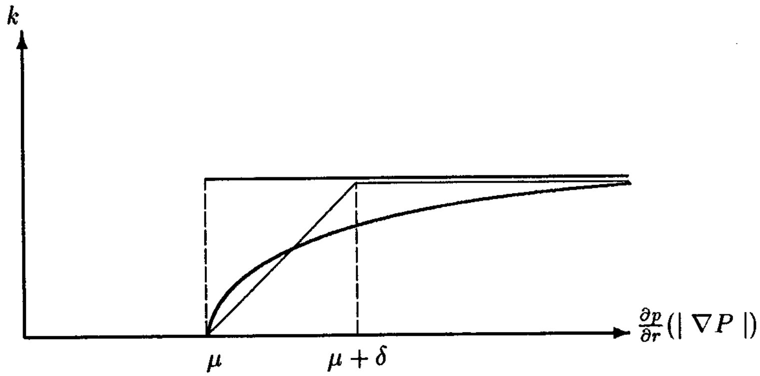

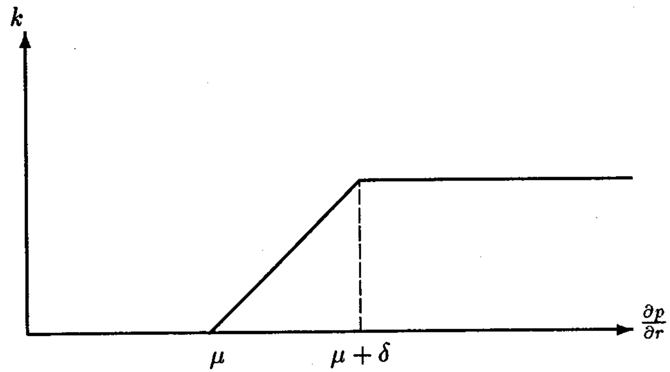

$$\begin{cases} 1 & \frac{\partial p}{\partial r} > \mu+\delta \\ \frac{1}{\delta}(\frac{\partial p}{\partial r}-\mu) & \\ 0 & \frac{\partial p}{\partial r} < \mu \end{cases}$$

$$\begin{cases} \frac{\partial p}{\partial t} = \frac{1}{r}\frac{\partial}{\partial r}(rk_\delta(\frac{\partial p}{\partial r})\frac{\partial p}{\partial r}) & 0 < r < \infty \\ p|_{t=0} = p_0 & \\ \lim\limits_{r\to 0}(r\frac{\partial p}{\partial r}) = Q & \end{cases}$$

How to get an approximate solution?

$$P(r,t) = p_0 - \frac{Q}{2}\int_{\frac{r^2}{4kt}}^{\infty}\frac{e^{-\lambda}}{\lambda}\,d\lambda \ (k \ll 1)$$

$$\frac{\partial p}{\partial r} = \frac{Qr}{4kt}\frac{4kt}{r^2}e^{-\frac{r^2}{4kt}} = \frac{Q}{r}e^{-\frac{r^2}{4kt}}$$

$$\frac{\partial p}{\partial r} > 0, \qquad \frac{\partial p}{\partial r} \searrow$$
$$\frac{\partial p}{\partial r} = \mu, \qquad \frac{Q}{r} e^{-\frac{r^2}{4kt}} = \mu$$
$$t = \frac{r^2}{\ln \frac{Q}{r\mu}} \qquad (r = r_f^0(t))$$

Find $\quad p = p_0(r, t)$

$$\begin{cases} \frac{\partial p}{\partial t} = \frac{1}{r}\frac{\partial}{\partial r}(r\frac{\partial p}{\partial r}) & 0 < r < \infty \\ p|_{t=0} = p_0 & \\ \lim\limits_{r \to 0}(r\frac{\partial p}{\partial r}) = Q & \\ p|_{r=r_f^0(t)} = p_0 & \end{cases}$$

(written by Jiang Lishang)

Flows in a Low Permeable and Compressible Medium

Huaxiong Huang
Department of Mathematics & Statistics, York University
Toronto, Canada M3J 1P3
Email: hhuang@yorku.ca

1 Introduction

Two problems on flows in low permeability reservoirs were posed to the 2^{nd} Shanghai Study Group with Industry, held at Fudan University, November 5-8, 2001. One of the problems is on radial axisymmetric flows with a threshold pressure gradient and the other is on radial flows in a compressible medium. The main objective of the exercise is to obtain exact or approximate solutions.

In the following, we summarize the discussion on one of the two problems, flows in a slightly compressible medium. The sub-group is consisted of A. Fitt, Y. He, H. Huang, L. Jiang, C. Please, F. Song, X. Ye and J. Yue.

2 Radial Flows in a Compressible Medium

Consider the radial axisymmetric flow in a compressible porous medium in a domain $r \geq 1$ described by the following initial-boundary value problem:

$$\begin{aligned} \frac{\partial u}{\partial t} &= \frac{u}{r}\frac{\partial}{\partial r}\left(r\frac{\partial u}{\partial r}\right), \quad t>0, \ r>1 && (1)\\ \frac{\partial u}{\partial r} &= \beta + \frac{1}{u}\frac{\partial u}{\partial t}, \quad r=1 && (2)\\ \frac{\partial u}{\partial r} &= 0, \quad r \to \infty && (3)\\ u &= 1, \quad t=0 && (4) \end{aligned}$$

where $u = \exp(-\beta p)$ and p is the pressure. The permeability of the medium is assumed to be a function of p in the form of $K = K_0 \exp(-\beta p)$ with β being a (positive) parameter. The initial-boundary value problem (1)-(4) can be derived from the conservation of mass and the Darcy's law and the details can be found in [5]. Here we consider slightly compressible media where β is small. We note that $u \to 1$ as $\beta \to 0$.

Because of the non-linear nature of the equation, the exact solution may not exist for this problem. So the rest of the discussion is on approximate solutions. In particular, we focus on the following questions: Can we obtain a practically useful approximate solution and how does the approximate solution compare to numerical solutions? It is worth pointing out that the the boundary condition (2) and the initial condition (4) are incompatible at $r = 1$ and $t = 0$, which is likely to cause the deterioration of accuracy in the numerical solution for small time t. It was also noted that the original boundary condition (2) at the well $r = 1$ may be replaced by the following condition

$$\frac{\partial u}{\partial r} = \beta, \quad r = 1 \tag{5}$$

assuming that the medium inside the well is incompressible.

In order to simplify the computation, we will first study two model problems in Cartesian coordinates where straightforward comparison can be made between numerical and approximate (asymptotic) solutions. Discussion on the radial flows will be given afterwards.

2.1 A model problem in Cartesian coordinates

We consider the following problem in Cartesian coordinates

$$\frac{\partial u}{\partial t} = u\frac{\partial^2 u}{\partial x^2}, \quad t > 0, \ x > 0 \tag{6}$$

$$\frac{\partial u}{\partial x} = \beta, \quad x = 0 \tag{7}$$

$$\frac{\partial u}{\partial x} = 0, \quad x \to \infty \tag{8}$$

$$u = 1, \quad t = 0 \tag{9}$$

2.1.1 Regular perturbation

We look for approximate solution via regular perturbation method, by expanding the solution into an asymptotic series of β

$$u = 1 + \beta u^{(1)} + \beta^2 u^{(2)} + \cdots$$

At the first order, we have

$$\frac{\partial u^{(1)}}{\partial t} = \frac{\partial^2 u^{(1)}}{\partial x^2}, \quad t > 0, \ \ x > 0 \tag{10}$$

$$\frac{\partial u^{(1)}}{\partial x} = 1, \quad x = 0 \tag{11}$$

$$\frac{\partial u^{(1)}}{\partial x} = 0, \quad x \to \infty \tag{12}$$

$$u^{(1)} = 0, \quad t = 0. \tag{13}$$

The solution of this problem can be obtained using Laplace transform as

$$u^{(1)} = -2\sqrt{\frac{t}{\pi}} \exp\left(-\frac{x^2}{4t}\right) + x \mathrm{erfc}\left(\frac{x}{2\sqrt{t}}\right).$$

Obviously the solution is smooth for $t > 0$. However, the derivative $\partial^2 u^{(1)}/\partial x^2$ blows up as $1/\sqrt{t}$ on the boundary $x = 0$ as $t \to 0$.

The overall solution up to the first order of β is

$$u = 1 + \beta \left[-2\sqrt{\frac{t}{\pi}} \exp\left(-\frac{x^2}{4t}\right) + x \mathrm{erfc}\left(\frac{x}{2\sqrt{t}}\right)\right] + O(\beta^2).$$

2.1.2 Numerical method

We apply a standard finite volume method to our model problem. The semi-discrete equations can be written as

$$\frac{du_i}{dt} = \frac{2u_i}{x_{i+1} - x_{i-1}} \left(\frac{u_{i+1} - u_i}{x_{i+1} - x_i} - \frac{u_i - u_{i-1}}{x_i - x_{i-1}}\right), \quad t > 0 \tag{14}$$

for $i = 1, ..., N-1$ on a grid $0 \equiv x_0 < x_1 < \cdots < x_{N-1} < x_N \equiv x_\infty$ where the infinity domain is truncated by replacing ∞ with x_∞. The equations for $i = 0$ and $i = N$ can be derived using fictitious points x_{-1} and x_{N+1} and a discrete form of the boundary conditions (7) and (8).

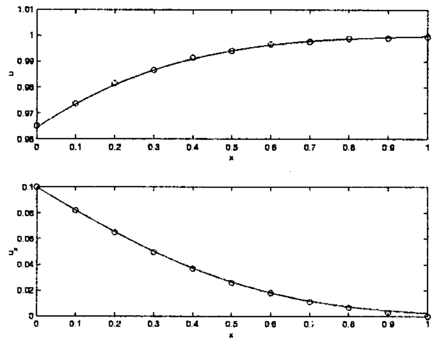

Figure 1: *Solutions at $t = 0.1$ in Cartesian coordinates using using boundary condition $\partial u/\partial x = \beta$ at $x = 0$. Solid line is for asymptotic solution and symbols are for the numerical solution on a uniform grid grid with $\delta x = 1$.*

It was shown in [3] for similar problems that the accuracy of the semi-discretization is determined by the grid size δx as well as the second derivative $\partial^2 u/\partial x^2$, which in our case is dominated by $\beta\partial^2 u^{(1)}/\partial x^2$ when β is small. In order to isolate the error due to spatial discretization, we use `ode45`, a Matlab [7] code which uses the Runge-Kutta method of order 4 to solve the system of ordinary differential equations (14).

2.1.3 Comparison of asymptotic and numerical solutions

In Figure 1, solution u and its derivative u_x are plotted for $t = 0.1$. (For the rest of the discussion, we choose $\beta = 0.1$.) It can be seen that the numerical solution, obtained on a uniform grid with $\delta x = 0.1$, is in good agreement with the asymptotic solution. However, for a smaller time $t = 0.001$, there exists visible difference between the

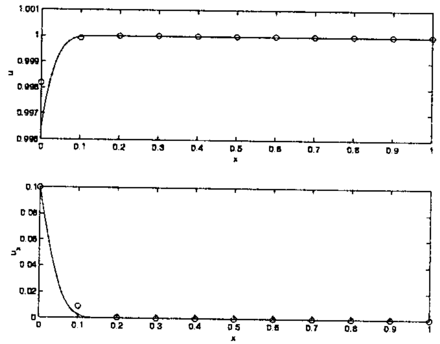

Figure 2: *Solutions at* $t = 0.001$ *in Cartesian coordinates using using boundary condition* $\partial u/\partial x = \beta$ *at* $x = 0$. *Solid line is for asymptotic solution and symbols are for the numerical solution on a uniform grid grid with* $\delta x = 1$.

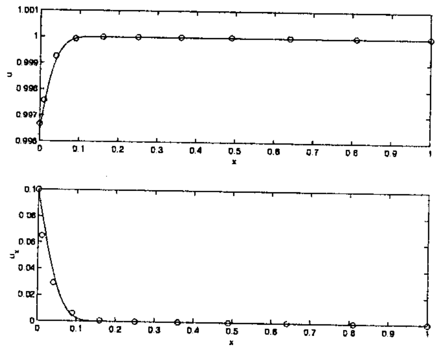

Figure 3: *Solutions at* $t = 0.001$ *in Cartesian coordinates using using boundary condition* $\partial u/\partial x = \beta$ *at* $x = 0$. *Solid line is for asymptotic solution and symbols are for the numerical solution on a non-uniform grid* $x_i = (i/N)^2$.

two solutions near $x = 0$ on the same grid, as shown in Figure 2. This is likely due to the lack of resolution near $x = 0$. To increase the resolution, one can refine the grid globally by using more grid points, or locally by using a non-uniform grid without increasing the number of grid points. It can be seen in Figure 3 that the numerical solution, obtained on a non-uniform graded mesh, agrees well with the asymptotic solution. In conclusion, the approximate solution obtained by regular perturbation is quite accurate even with only one correction. The numerical solution becomes less reliable for small time and grid refinement is necessary to maintain accuracy.

2.2 Model problem 2 in Cartesian coordinates

We now come back to the original boundary condition, but still in Cartesian coordinates and consider the following problem

$$\frac{\partial u}{\partial t} = u\frac{\partial^2 u}{\partial x^2}, \quad t > 0, \quad x > 0 \tag{15}$$

$$\frac{\partial u}{\partial x} = \beta + \frac{1}{u}\frac{\partial u}{\partial t}, \quad x = 0 \tag{16}$$

$$\frac{\partial u}{\partial x} = 0, \quad x \to \infty \tag{17}$$

$$u = 1, \quad t = 0 \tag{18}$$

We look for the approximate solution via regular perturbation method in a similar way

$$u = 1 + \beta u^{(1)} + O(\beta^2)$$

where

$$\frac{\partial u^{(1)}}{\partial t} = \frac{\partial^2 u^{(1)}}{\partial x^2}, \quad t > 0, \ x > 0 \tag{19}$$

$$\frac{\partial u^{(1)}}{\partial x} = 1 + \frac{\partial u^{(1)}}{\partial t}, \quad x = 0 \tag{20}$$

$$\frac{\partial u^{(1)}}{\partial x} = 0, \quad x \to \infty \tag{21}$$

$$u^{(1)} = 0, \quad t = 0. \tag{22}$$

Using Laplace transform we obtain

$$u^{(1)} = -\int_0^t e^{t-\tau} \operatorname{erfc}\left(\sqrt{t-\tau}\right) \operatorname{erfc}\left(\frac{1}{2}\frac{x}{\sqrt{\tau}}\right) d\tau.$$

The overall solution up to the first order of β is

$$u = 1 - \beta\left[\int_0^t e^{t-\tau} \operatorname{erfc}\left(\sqrt{t-\tau}\right) \operatorname{erfc}\left(\frac{1}{2}\frac{x}{\sqrt{\tau}}\right) d\tau\right] + O(\beta^2).$$

In Figure 4, we plotted the asymptotic and numerical solutions at $t = 0.1$. The computation was done on a uniform grid with $\delta x = 0.1$. It can be seen that the biggest error of u_x now occurs at $x = 0$. This can be seen more clearly from Figure 5 where $u_x(0,t)$ is plotted against t. It can be observed that the error increases as t decrease on a given grid. To improve accuracy, finer grid is needed near $x = 0$ as t becomes smaller. It is worth noting that even though the asymptotic solution is obtained for this case, it involves integrations which must be evaluated numerically. In this study, we have used Maple [6], a symbolic mathematical package and it takes a much longer time to find the asymptotic solution for a given x and t, compared to solving the equation numerically. Thus, its usefulness may be limited from practical point of view.

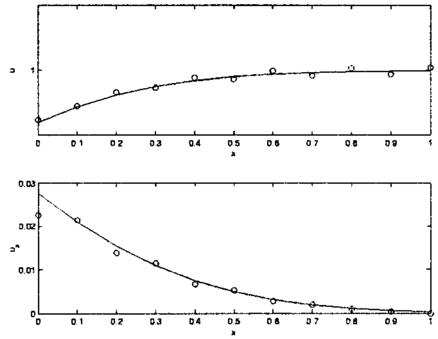

Figure 4: *Solutions at* $t = 0.1$ *in Cartesian coordinates using* $\partial u/\partial x = \beta + u^{-1}\partial u/\partial t$ *at* $x = 0$. *Solid line is for asymptotic solution and symbols are for the numerical solution on a uniform grid* $\delta x = 1$.

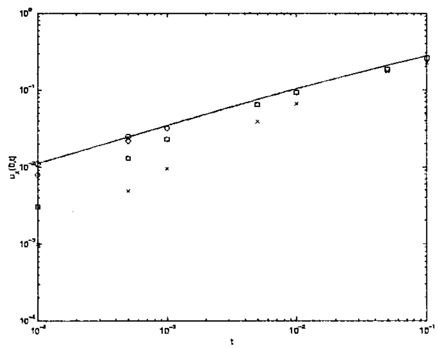

Figure 5: *Solutions at* $t = 0.001$ *in Cartesian coordinates using* $\partial u/\partial x = \beta + u^{-1}\partial u/\partial t$ *at* $x = 0$. *Solid line is for asymptotic solution and symbols are for the numerical solutions. Cross's are for numerical solution on a uniform grid. Non-uniform graded mesh* $x_i = (i/N)^\kappa$ *is used for other computation: squares for* $\kappa = 1.5$*; diamonds for* $\kappa = 2$ *and circles for* $\kappa = 2.5$.

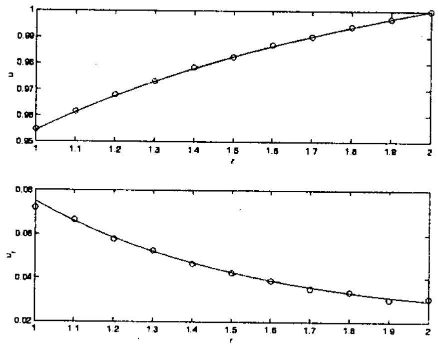

Figure 6: *Solutions for radial flows at* $t = 1$*: solid line is for asymptotic solution; symbols are for the numerical solution on a uniform grid with* $\delta x = 0.1$.

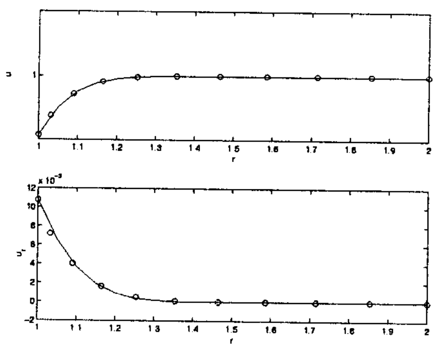

Figure 7: *Solutions for radial flows at* $t = 0.01$*: solid line is for asymptotic solution; symbols are for the numerical solution on a non-uniform grid* $r_i = a + (i/N)^{1.5}(b - a)$.

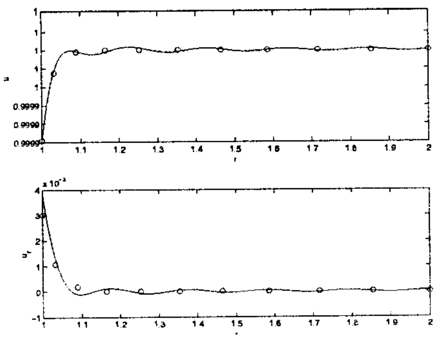

Figure 8: *Solutions for radial flows at* $t = 0.001$*: solid line is for asymptotic solution; symbols are for the numerical solution on a non-uniform grid* $r_i = a + (i/N)^{1.5}(b-a)$.

2.3 Radial flows

We now briefly discuss our original problem (1)-(4). Using regular perturbation, we have $u = 1+\beta u^{(1)}+O(\beta^2)$ where $u^{(1)}$ is the solution of the following problem

$$\frac{\partial u^{(1)}}{\partial t} = \frac{1}{r}\frac{\partial}{\partial r}\left(r\frac{\partial u^{(1)}}{\partial r}\right), \quad t>0, \ r>1 \tag{23}$$

$$\frac{\partial u^{(1)}}{\partial r} = 1+\frac{\partial u^{(1)}}{\partial t}, \quad r=1 \tag{24}$$

$$\frac{\partial u^{(1)}}{\partial r} = 0, \quad r\to\infty \tag{25}$$

$$u^{(1)} = 0, \quad t=0. \tag{26}$$

The solution of this problem may be obtained using Laplace transform in an integral form, as in the case of the Cartesian coordinates discussed earlier. However, since it is computationally expensive to compute these integrals and our numerical solution is obtained on a finite domain, we will restrict our domain to an anulus: $1 = a \le r \le b$.

The solution v for the unsteady heat equation on an anulus $a \le r \le b$ with the following boundary conditions

$$\begin{aligned} k_1 \frac{\partial v}{\partial t} + k_2 \frac{\partial v}{\partial r} + k_3 v &= k_4, \quad r = a, \\ k_1' \frac{\partial v}{\partial t} + k_2' \frac{\partial v}{\partial r} + k_3' v &= k_4', \quad r = b, \end{aligned}$$

is given by Jaeger [4], which was reproduced in [2] as

$$\begin{aligned} v = & \frac{ak_4[k_2' - bk_3' \log(r/b)] - bk_4'[k_2 - ak_3 \log(r/a)]}{ak_3k_3' - bk_2k_3' - abk_3k_3' \log(a/b)} \\ & -\pi \sum_{n=1}^{\infty} e^{-\alpha_n^2 t} F(\alpha_n) U_0(r, \alpha_n) \{k_4[A_n' J_0(b\alpha_n) - k_2' \alpha_n J_1(b\alpha_n)] \\ & -k_4'[A_n J_0(a\alpha_n) - k_2 \alpha_n J_1(a\alpha_n)]\}, \end{aligned}$$

where

$$A_n = k_3 - k_1 \alpha_n^2, \quad A_n' = k_3' - k_1' \alpha_n^2, \quad B = k_2 + \frac{2k_1}{a}, \quad B' = k_2' + \frac{2k_1'}{b},$$

$$\begin{aligned} F(\alpha_n) = & \left\{A_n' J_0(b\alpha_n) - k_2' \alpha_n J_1(b\alpha_n)\right\} \Big/ \\ & \left\{[A_n' J_0(b\alpha_n) - k_2' \alpha_n J_1(b\alpha_n)]^2 (A_n^2 + k_2 B \alpha_n^2) \right. \\ & \left. -[A_n J_0(a\alpha_n) - k_2 \alpha_n J_1(a\alpha_n)]^2 (A_n'^2 + k_2' B' \alpha_n^2)\right\}, \\ U_0 = & J_0(r\alpha_n)[A_n Y_0(a\alpha_n) - k_2 \alpha_n Y_1(a\alpha_n)] \\ & -Y_0(r\alpha_n)[A_n J_0(a\alpha_n) - k_2 \alpha_n J_1(a\alpha_n)], \end{aligned}$$

J_0, J_1, Y_0 and Y_1 are the Bessel functions of the first and second kinds, respectively and the eigenvalues α_n are the positive roots of

$$\begin{aligned} & [(k_3 - k_1\alpha^2) J_0(a\alpha) - k_2 \alpha J_1(a\alpha)][(k_3' - k_1'\alpha^2) Y_0(a\alpha) - k_2' \alpha Y_1(a\alpha)] \\ & -[(k_3' - k_1'\alpha^2) J_0(b\alpha) - k_2' \alpha J_1(b\alpha)][(k_3 - k_1\alpha^2) Y_0(b\alpha) - k_2 \alpha Y_1(b\alpha)] \\ & = 0 \end{aligned}$$

On boundary $r = b$, we will use $u^{(1)} = 0$ as the boundary condition since $\partial u^{(1)}/\partial r = 0$ is incompatible with the condition $\partial u^{(1)}/\partial r = 1 + \partial u^{(1)}/\partial r$ on $r = a$. (Alternatively, we can use $\partial u^{(1)}/\partial r = k_4' \neq 0$.) Therefore, we have $k_1 = -1$, $k_2 = k_4 = k_3' = 1$, $k_3 = k_1' = k_2' = k_4' = 0$. And the first ten positive eigenvalues computed using Maple are

$$\alpha_n = 1.0274,\ 3.4231,\ 6.4302,\ 9.5236,\ 12.6407,$$
$$15.7675,\ 18.8992,\ 22.0337,\ 25.1700,\ 28.3075$$

for $a = 1$ and $b = 2$.

In Figures 6-8, we have plotted the asymptotic solution and the numerical solution at $t = 1$, 0.01 and 0.001. The numerical solution (symbol) is obtained using a finite volume discretization in r. The time integration is again done using the Matlab code `ode45`. The uniform grid is used for $t = 1$ but a graded mesh $r_i = 1 + (i/N)^{1.5}$ is used for t=0.01 and 0.001. It is clear from the figures that the asymptotic solution agrees with the numerical solution well for $t = 1$ and 0.01, with the infinite series is truncated at $n = 10$. At $t = 0.001$, the asymptotic solution becomes oscillatory, which indicates that more eigenvalues need to be included in the expansion. In fact, it will be more efficient to seek an expansion of the solution valid for $t \ll 1$. However, we will not discuss the issue any further in this report.

3 Conclusion

In this report we have investigated radial flows in a low permeable and slightly compressible medium. Regular perturbation method is used to obtain approximate solution when the compressibility parameter β is small. It is shown that in general the asymptotic solution with only one correction term agrees well with the numerical solution. However, approximate solution obtained here becomes less accurate or more expansive to compute for small time. Thus, it may be desirable to expand solution into a form suitable for $t \ll 1$ since it will be computationally more efficient. Such solutions have been obtained for the heat equations and some of them can be found in [1, 2].

When $t \to 0$, numerical solution also becomes less accurate on a fixed grid due to the incompatibility between the boundary and initial conditions at $t = 0$. A non-uniform graded mesh produces more accurate solutions but we have not conducted a systematic study on the effect of a mesh refinement strategy.

References

[1] H.S. Carslaw and J.C. Jaeger, Conduction of Heat in Solids, Oxford (1947).

[2] J. Crank, Mathematics of Diffusion, Oxford, sec. 5.42 (1956).

[3] H. Huang and B.R. Wetton, *Journal of Computational Physics* 126:468 (1996).

[4] J.C. Jaeger, *Proc. Roy. Soc. N.S.W.* 74:342 (1940).

[5] X. Kong, Advanced Porous Media Flows (1990's).

[6] Waterloo Maple, Version 6 (2000). `http://www.maple.com`.

[7] Matlab Release 12, Student Version (1999). `http://www.mathworks.com`.

[8] F. Song, Ph.D. Dissertation (1999).